

引用格式: GUO Jia-wei, JIA Kai, YANG Feng, *et al.* Simulation and Experiment of Thermal Characteristics of a Jet Cooling Composite Ceramic Thin-disk Laser[J]. *Acta Photonica Sinica*, 2020, **49**(3): 0314001
郭嘉伟, 贾凯, 杨峰, 等. 喷流冷却复合陶瓷薄片激光器的热特性仿真分析及实验研究[J]. *光子学报*, 2020, **49**(3): 0314001

喷流冷却复合陶瓷薄片激光器的热特性 仿真分析及实验研究

郭嘉伟¹, 贾凯¹, 杨峰^{1, 2}, 彭春¹, 汪晓聪¹, 刘晓旭¹,
韩聚洪¹, 荣克鹏¹, 安国斐¹, 蔡和¹, 王澈¹

(1 西南技术物理研究所, 成都 610041)

(2 四川大学 电子信息学院, 成都 610065)

摘 要: 为分析喷流冷却复合陶瓷薄片激光器的热特性, 设计用于冷却复合陶瓷薄片的喷流冷却系统。利用湍流换热理论和计算流体力学仿真方法建立喷流冷却复合陶瓷薄片激光器的流固耦合热仿真模型, 定义评价其冷却能力和冷却均匀性的定量参数。根据该仿真模型得到喷流冷却系统的最优设计参数, 并进行实验验证。使用 163 孔喷板, 流量为 0.2 kg/s, 入口温度为 20 °C, 在 1 200 W 泵浦时获得 359 W 激光输出功率, 并测得复合陶瓷薄片上表面的最高温度为 92 °C。激光输出功率与复合陶瓷薄片上表面温度均与泵浦功率呈近似正线性关系, 且温度的实验值与仿真值相符度较高。

关键词: 激光器; 薄片; 喷流冷却; Nd: YAG; 复合陶瓷; 计算流体力学

中图分类号: TN248.1

文献标识码: A

doi: 10.3788/gzxb20204903.0314001

Simulation and Experiment of Thermal Characteristics of a Jet Cooling Composite Ceramic Thin-disk Laser

GUO Jia-wei¹, JIA Kai¹, YANG Feng^{1, 2}, PENG Chun¹, WANG Xiao-cong¹, LIU Xiao-xu¹,
HAN Ju-hong¹, RONG Ke-peng¹, AN Guo-fei¹, CAI He¹, WANG You¹

(1 Southwest Institute of Technical Physics, Chengdu 610041, China)

(2 College of Electronics and Information Engineering, Sichuan University, Chengdu 610065, China)

Abstract: In order to analyze the thermal characteristics of a jet cooling thin-disk composite ceramic laser, the jet cooling device for a composite ceramic thin-disk laser is designed. A systematic simulation model is developed by using the turbulent heat transfer theory and computational fluid dynamics method. Two evaluation parameters are defined for the cooling capacity and uniformity of the designed jet cooling device. The optimal parameters of the jet cooling device are obtained by using the simulation model, and a verification experiment is carried out afterward. In the experiment, a jet plate with 163 holes is adopted, the inlet coolant flow rate and temperature are set to be 0.2 kg/s and 20 °C, respectively. When the pump power is raised to 1 200 W, the output power of 359 W has been achieved, and the maximal temperature on the upper surface of the thin-disk composite ceramic detected by a thermal camera has reached to 92 °C. It is also demonstrated that there have been approximate positive linear relationships

Foundation item: National Key Research and Development Program of China (No.2017YFB0405100)

First author: GUO Jia-wei (1986—), male, senior engineer, Ph.D. degree candidate, mainly focuses on thermal effect of solid-state laser. Email: lcl-330@163.com

Supervisor (Contact author): WANG You (1966—), male, professor, Ph.D. degree, mainly focuses on alkali vapor laser and solid-state laser. Email: youwang_2007@aliyun.com

Received: Nov.15, 2019; **Accepted:** Jan.2, 2020

<http://www.photon.ac.cn>

between the pump power and both the output power and the temperature on the upper surface of the thin-disk of composite ceramic, and the experimental temperature value shows good agreement with simulated value.

Key words: Laser; Thin-disk; Jet cooling; Nd : YAG; Composite ceramic; Computational fluid dynamics

OCIS Codes: 140.3580; 010.7060; 120.6810; 140.5680; 160.3380

0 Introduction

High-powered Laser Diode (LD)-pumped solid-state lasers are very important light sources for many applications such as material processing, industrial cleaning, and national defense, etc^[1-4]. However, there are some disadvantages of a LD-pumped solid-state laser such as relatively unsatisfied beam quality at even higher output power, which mainly results from the serious thermally-induced birefringence and thermally-induced lens of a laser medium^[5-7].

LD-pumped thin-disk solid-state lasers offer a large ratio of diameter to thickness of a laser medium. The laser beam transfers along the axial direction, which is vertical to the surface of the laser disk. An end surface cooling configuration of a thin-disk solid-state laser offers the short distance of heat conduction and a large ratio of the cooling area to the heat generation volume, which can enormously reduce the operation temperature of a laser medium. If the pumping and cooling distributions of a thin-disk solid-state laser are uniform, the heat flux will only exist along the axial direction and the temperature gradient will not exist along the radial and tangential directions. The thermally-induced optical distortion can be therefore deduced of a laser medium^[8-9]. Thus, a high-performance and uniform cooling configuration is required for a thin-disk solid-state laser with the high output power and good beam quality.

In the jet cooling scheme, the flowing coolant is assumed to directly contact with a laser medium in order to generate the turbulent heat transfer, which offers some advantages of simple technique and less installed stress. There are several research works about the jet cooling thin-disk laser. In 2011, VRETENAR N et al. investigated the thermal effects of a jet impingement cooling capped YAG/Yb:YAG thin-disk laser^[10]. In 2012, SARAVANI M et al. investigated the impact of the substrate thickness and material thermal conductivity effects on temperature distribution and thermal stress of thin disk laser through analyzing heat flow in jet impingement cooling system^[11]. In 2014, GUO J et al. used a simulated heat source to analyze the performance of the jet cooling technology on a thin-disk laser^[12]. In 2016, SHAO N et al. analyzed the core factor of cooling effect of jet array impingement unit of disk-laser crystal module^[13]. In addition, there is almost no intermediate thermal resistance between the coolant and the heat medium, and the optical films cannot be directly destroyed^[14-15].

As a novel lasing material, the transparent ceramic has numerous advantages compared with laser crystals for high power solid-state lasers. The physical features of pure ceramic, doped ceramic, and composite ceramic are very close to laser crystals^[16-18]. A high-performance and uniform cooling for a composite ceramic can be achieved by the design optimization of the jet cooling configuration.

In this paper, we carried out the theoretical analyses, schematic design, simulation, and experiment for a jet cooling thin-disk composite ceramic laser. The structure of a jet cooling device for a thin-disk composite ceramic laser is designed, and a systematic simulation model is developed by using the turbulent heat transfer theory and Computational Fluid Dynamics (CFD) method. Two evaluation parameters for cooling capacity and uniformity of the jet cooling device are defined. The structural parameters of a jet cooling device are optimized by the simulation, and a verification experiment for thermal and power Input-Output (I-O) characteristics has been carried out afterward. At last, we compare the simulated and experimental temperatures of the upper surface of a thin-disk composite ceramic, and give some conclusions.

1 Configuration and theory

The configuration diagram of a jet cooling thin-disk composite ceramic laser is shown in Fig.1. Here, a V-shaped plano-concave resonator has been adopted, the reflectivity of the output coupler is 85%, the

curvature radius of the reflective mirror is 5 m, and the resonator length is 1.2 m. The reshaped 808 nm LD pump beam is evenly injected into the ceramic disk by some projection lenses, and the unabsorbed pump light can be reflected by the spherical reflector to achieve the 4-pass pumping. The pumping plane ($X-Z$) and lasing plane ($Y-Z$) of the light are perpendicular each other. The pumping plane is in the horizontal direction and the lasing plane is in the vertical direction, respectively.

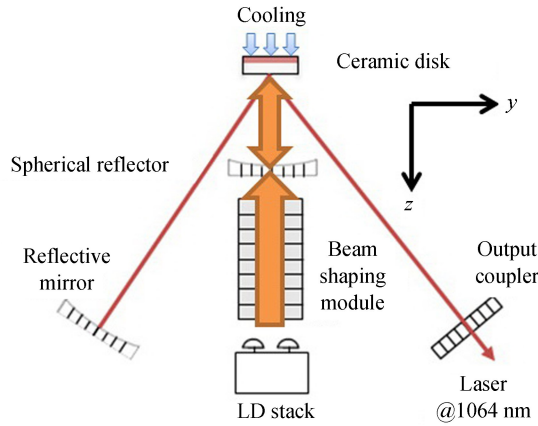


Fig.1 Configuration diagram of a jet cooling thin-disk composite ceramic laser

The composite ceramic YAG/Nd : YAG disk consists of 4 mm-thick pure YAG and 2 mm-thick Nd : YAG with the doping concentration of 1.0 at.%. The configuration of a ceramic disk is shown in Fig.2. One surface of the composite ceramic irradiated by the pump light is coated with Anti-Reflective (AR) films@ 808 and 1 064 nm. The other surface is coated with High-Reflective (HR) films@808 and 1 064 nm, and the lateral side is deliberately roughened in order to avoid Amplified Spontaneous Emission (ASE).

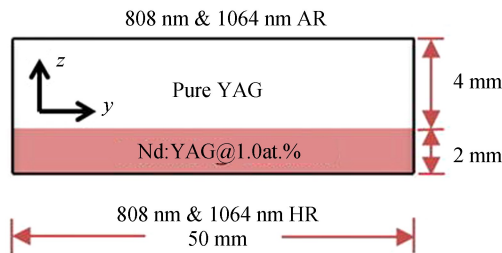


Fig.2 Schematic illustration of a large diameter composite ceramic

The jet cooling configuration of a thin-disk composite ceramic laser is shown in Fig. 3. The coolant is forced to flow through a jet plate with some holes by a water pump. Each hole is functioned like a liquid nozzle , and has a specific shape which will be illustrated in the next section . These holes are specifically

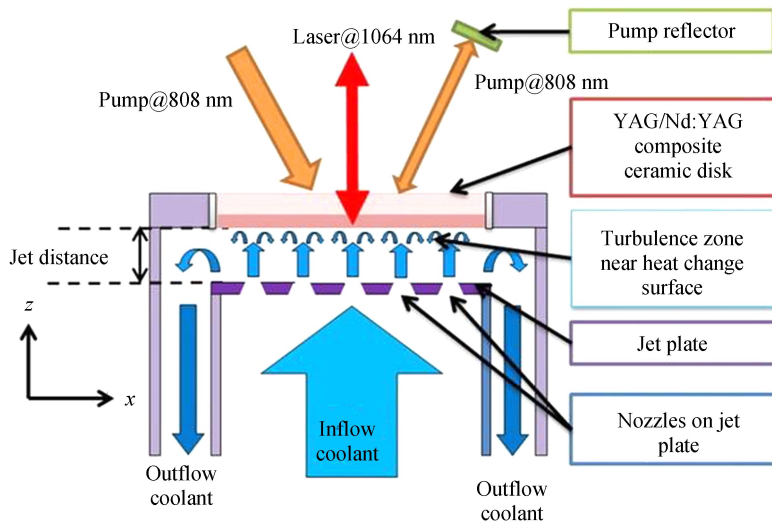


Fig.3 Configuration of jet cooling

arranged to distribute on a jet plate. The coolant passes through these nozzles and jets towards the heat transfer surface (i.e., the lower surface of the composite ceramic thin-disk) with a very high velocity. Thus, severe turbulent disturbance can be formed. The cooling capacity will be evidently improved because the heat transfer capacity of turbulence is much higher than that of laminar flow and the thickness of the coolant boundary layer near the heat transfer surface is reduced due to the severe turbulent disturbance^[19].

The Convective Heat Transfer Coefficient (CHTC) is adopted to quantitatively represent the cooling performance of coolant on the heat transfer surface^[19]. A CHTC ($\text{W}/\text{m}^2/\text{C}$) is defined as the ratio of the heat flux, which is perpendicular to the heat transfer surface, to the difference between the temperatures of the heat transfer surface and coolant as expressed by

$$h_{\text{interface}} = \frac{\Phi_{q_interface}}{T_{\text{interface}} - T_{\text{coolant}}} \quad (1)$$

where $h_{\text{interface}}$ is the CHTC of the heat transfer surface, $\Phi_{q_interface}$ is the heat flux (W/m^2) perpendicular to the heat transfer surface, $T_{\text{interface}}$ and T_{coolant} ($^{\circ}\text{C}$) are the temperatures of the heat transfer surface and coolant, respectively.

According to Fourier heat conduction law, the steady-state heat conduction equation with constant physical property of solid material with internal heat source can be expressed by Poisson equation

$$\nabla^2 T + \frac{\Phi}{k} = 0 \quad (2)$$

where ∇^2 is the Laplace operator, T ($^{\circ}\text{C}$) is the temperature of solid material, Φ (W/m^3) is the generated heat density of solid material, k ($\text{W}/\text{m}/\text{C}$) is the thermal conductivity of solid material, respectively.

If Φ , k , and T_{coolant} are acquired, and all surfaces except the heat transfer surface are assumed to be adiabatic, the temperature distribution of a thin-disk composite ceramic $T_{\text{ceramic}}(x, y, z)$ will be evaluated by Eq. (2) with the Robin boundary condition which is the CHTC distribution on the heat transfer surface. Thus, the evaluation of the CHTC distribution on the heat transfer surface is the key point in analyzing the thermal characteristics of a jet cooling thin-disk composite ceramic laser.

2 Simulation model and discussions

2.1 Simulation model

In this subsection, a systematic simulation model is established to explore the thermal characteristics of a jet cooling thin-disk composite ceramic laser by using a CFD software of ANSYS-CFX as shown in Fig.4. We undertake simulations on 10 patterns of the jet plate as shown in Fig.5. The shape of all holes on the jet plate is top-flatted cone, and the distribution of holes on a jet plate obeys a regular hexagonal arrangement pattern. The jet distance between the lower surface of a composite ceramic thin-disk and the outlet of holes is 1 mm as shown in Fig.3^[12]. To ensure that the entire heat transfer surface can be efficiently cooled, the size of the hole array on the jet plate is a little larger than the diameter of the composite ceramic thin-disk. Due to the symmetry of geometry and boundary conditions of our simulation model on X-Z and Y-Z planes, the mesh quantity can be reduced to 1/4 of the original one for the purpose

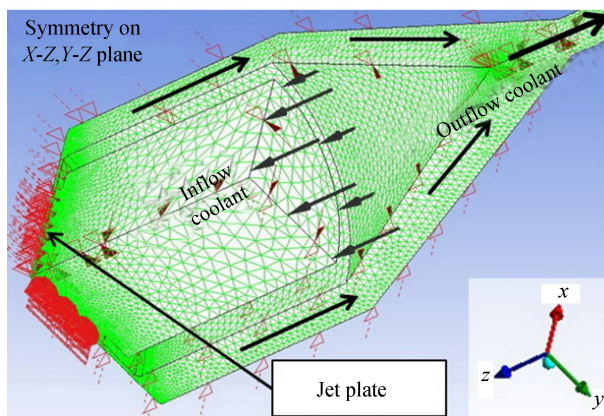


Fig.4 Schematic illustration of the thermal simulation of a jet cooling thin-disk composite ceramic laser

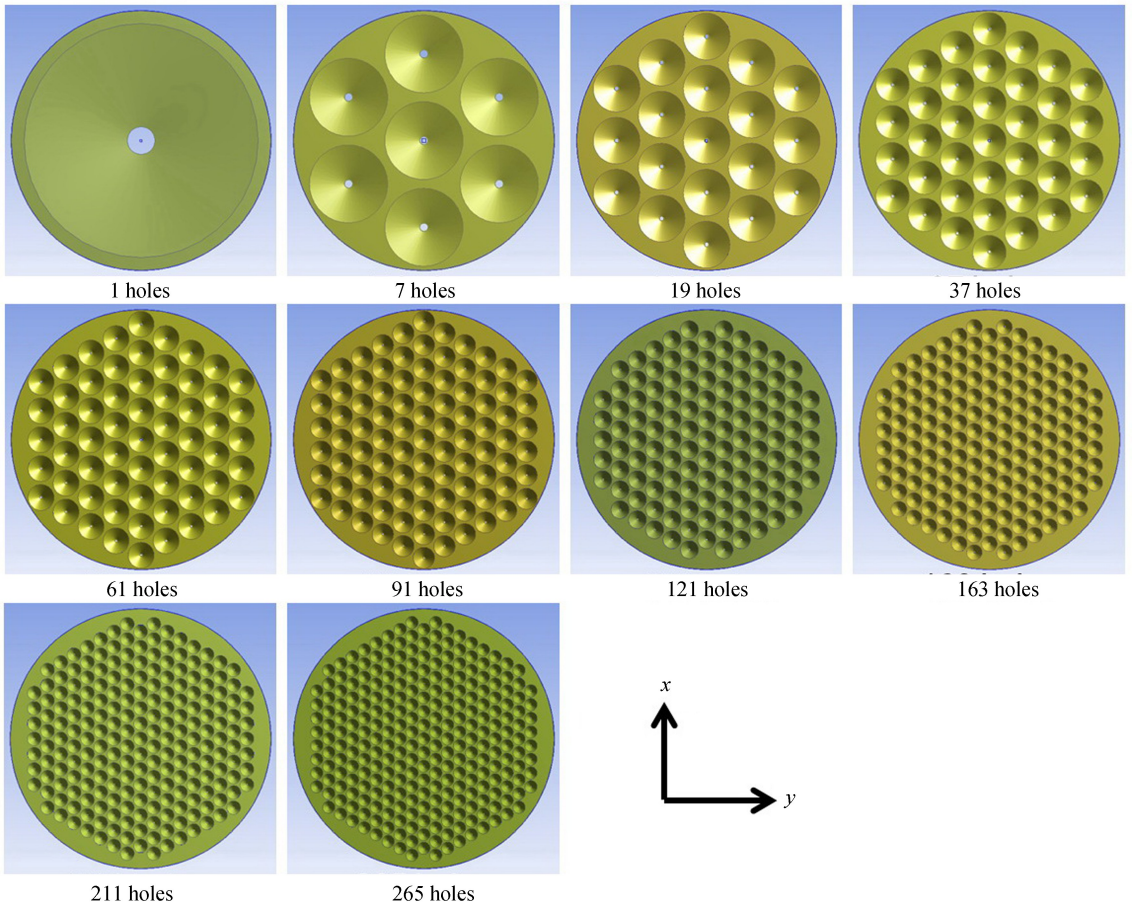


Fig.5 Geometric configurations of 10 kinds of jet plates with different holes

of saving the computation time. The sizes of the meshes near the hole outlet and heat transfer surface are set to 1/10 of the diameter of hole outlets and 0.2 mm, respectively.

Shear-Stress Transport (SST) turbulence model is adopted to calculate the turbulence and boundary layer characteristics near the heat transfer surface precisely^[20].

The distribution of the CHTC on the heat transfer surface is not uniform. The area weighted average convective heat transfer coefficient ($h_{AVE_interface}$) is defined to evaluate the cooling capacity of a jet cooling device on the heat transfer surface as expressed by

$$h_{AVE_interface} = \frac{\iint_A h_{interface}(x,y) dx dy}{A} \quad (3)$$

where A is the area of the heat transfer surface.

To evaluate the cooling uniformity of a jet cooling device on the heat transfer surface, the coefficient of variation of CHTC (C_{V_CHTC}) is defined by the ratio of the standard deviation of the CHTC distribution to the $h_{AVE_interface}$, as expressed by

$$C_{V_CHTC} = \frac{\sqrt{\frac{1}{A} \iint_A [h_{interface}(x,y) - h_{AVE_interface}]^2 dx dy}}{h_{AVE_interface}} \quad (4)$$

The cooling capacity increases with the $h_{AVE_interface}$, and the cooling uniformity decreases as the C_{V_CHTC} increases.

2.2 Results and discussions

In this subsection, the cooling capacity and uniformity of a jet cooling device are evaluated by a simulation model as described in subsection 2.1. We consider that the equal flow resistance standard is relatively suitable for the comparison of 10 kinds of jet plates with different number of holes. The outlet

diameters of 10 kinds of jet plates have been carefully adjusted to ensure that the coolant pressure differences for all jet plates are the same. Note that the flow rate of coolant passing through the jet plates are assumed to be the same value of 0.2 kg/s. Pure water is adopted as the coolant with the temperature of 20 °C. The coolant pressure difference are therefore calculated as about 2.1 atm. Table 1 lists the outlet diameters of holes on 10 different jet plates after a series of adjustment. Note that the holes on the jet plate must exhibit some special discrete number because of the geometric limitation (i.e. 1, 7, 19, 37...). The thicknesses of these jet plates are all 2 mm. The inlet diameters of holes on these jet plates are equal to 90% of the distances between the centers of adjacent holes for each jet plate.

Table 1 Outlet diameters of holes on 10 different jet plates

Number of holes on a jet plate	1	7	19	37	61	91	121	163	211	265
Outlet diameters of holes/mm	5,300	1,550	0,910	0,650	0,500	0,407	0,350	0,300	0,263	0,233

Fig.6 illustrates the CHTC distributions of 10 different jet plates by using the outlet diameters of holes as listed in Table 1. From the figure, we can see that the CHTC distribution patterns of 10 different jet plates are very similar to the distribution patterns of holes on 10 different jet plates as shown in Fig.5.

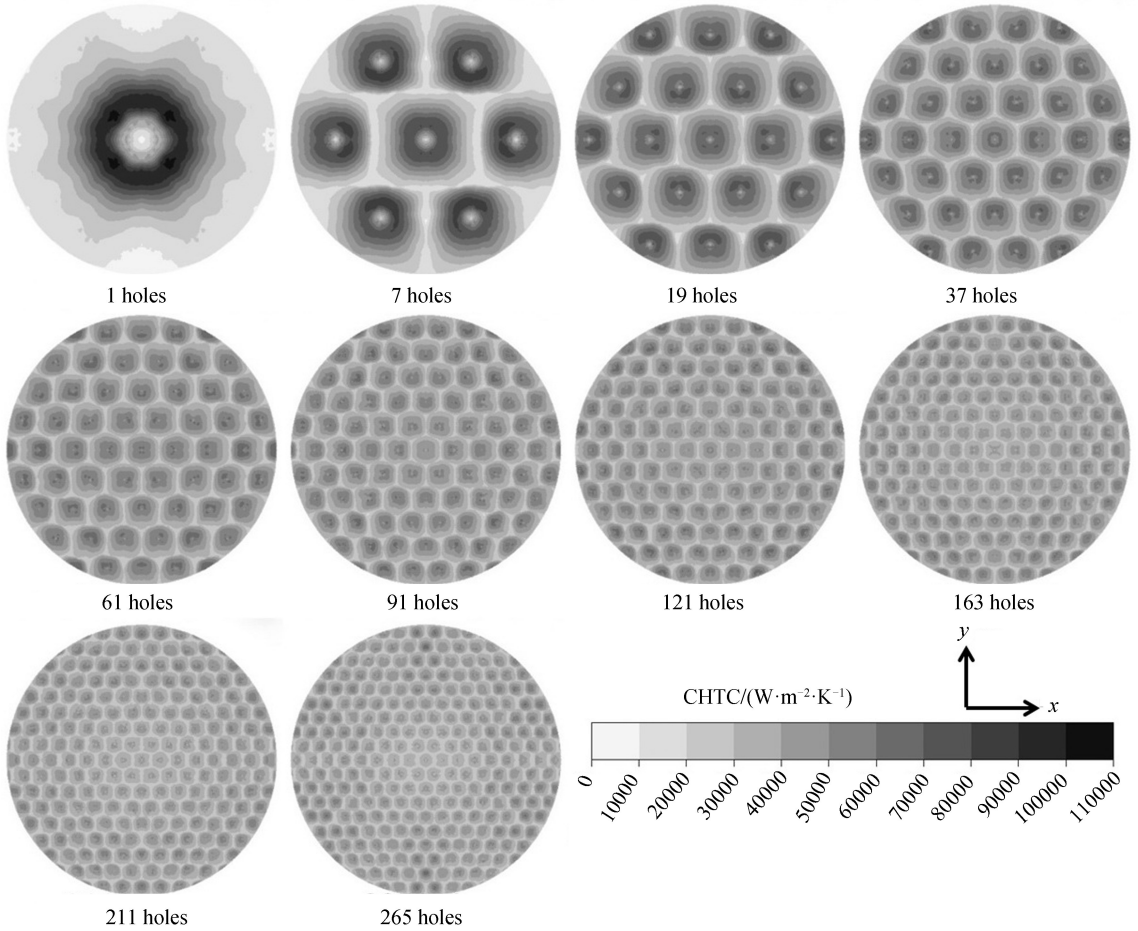


Fig.6 CHTC distributions for 10 kinds of jet plates with different holes

Fig.7 illustrates the $h_{AVE_interface}$ and C_{V_CHTC} of 10 different jet plates. When the jet plate of a larger number of holes is adopted, the $h_{AVE_interface}$, which represents the cooling capacity, first increases to the maximum when the number of holes on a jet plate is 19, and then slowly decreases. It means that the jet plate with 19 holes has the best cooling capacity. The C_{V_CHTC} , which represents the deterioration of cooling uniformity, first decreases to the minimum when the number of holes on a jet plate is 211, and then slowly increases with the hole number. It means that the jet plate with 211 holes has the best cooling uniformity.

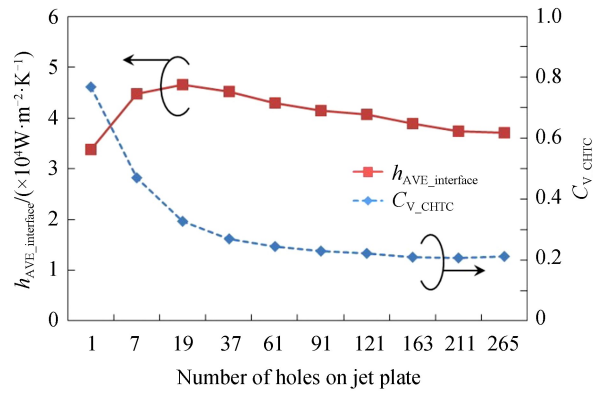


Fig.7 $h_{AVE_interface}$ and C_{V_CHTC} for 10 kinds of jet plates with different holes

From Table 1, the outlet diameters of 163 and 211 holes are respectively 0.300 mm and 0.263 mm. According to the machining experiences, it is extremely difficult to drill a lot of holes with the diameter less than 0.3 mm on a 2 mm-thick stainless steel jet plate with the tolerance of 0.001 mm. Moreover, the C_{V_CHTC} for 211 holes is merely 1.49% lower than that for 163 holes. Therefore, it is wise to adopt a configuration with 163 holes rather than one with 211 holes. The value of $h_{AVE_interface}$ for 163 holes is 83.58% of that for 19 holes, and the value of C_{V_CHTC} for 163 holes is 64.51% of that at 19 holes. The configuration with 19 holes is the best with the highest cooling capacity among 10 cases. On the other hand, the configuration with 163 holes is the best with the best cooling uniformity. Thus, the jet plate with 163 holes, whose relatively low cooling capacity can be accepted from the viewpoint of engineering, is thought to be optimal for a high-powered jet cooling thin-disk composite ceramic laser.

3 Experiments and results

An experiment for verifying the jet cooling thin-disk composite ceramic laser has been carried out with the configuration and parameters discussed in Sections 1 and 2. Fig.8 shows the photographs of a jet plate with 163 holes and a thin-disk composite ceramic.

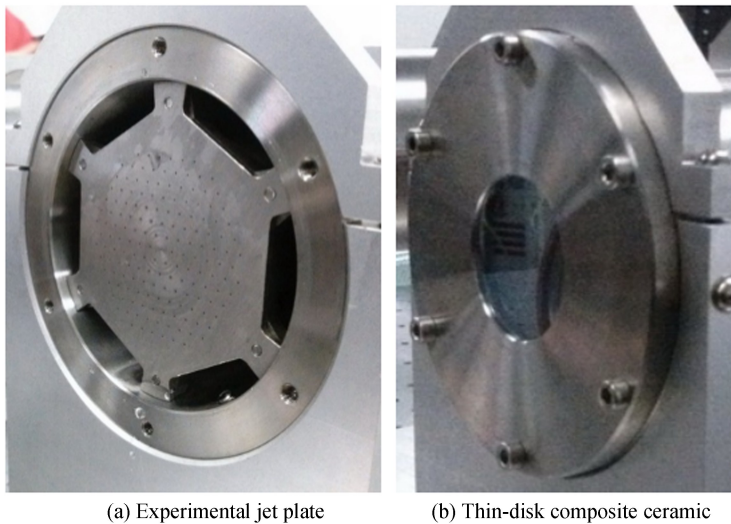


Fig.8 Photographs of an experimental jet plate and a thin-disk composite ceramic

In Fig.9, the simulated and detected maximal and minimal temperatures on the upper surface of a jet cooling composite ceramic thin-disk, and the experimental laser output power are represented as functions of the pump power, respectively. The output power linearly increases with the pump power and reaches to the maximum of 359 W at 1 200 W pump power with the optical-optical conversion efficiency of 29.2%. The simulation and experiment values are much closed to each other for both the maximal and the minimal temperatures in Fig. 9. One can observe that both of them linearly increase with the pump power.

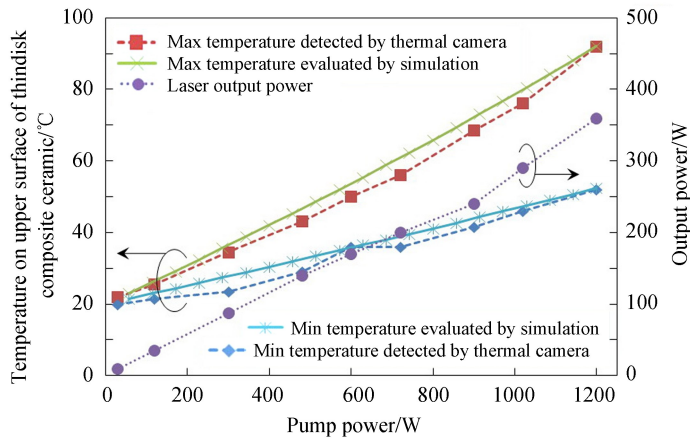


Fig.9 The maximal and minimal temperatures on the upper surface of a jet cooling thin-disk composite ceramic and the output power versus the pump power

Fig.10 shows the temperature distributions on the upper surface of composite ceramic thin-disk, which is pumped by 1 200 W LDs, detected by a thermal camera and evaluated by the simulation, respectively. As a hexagonal kaleidoscope and several cylindrical lenses are adopted to obtain a homogeneous pump beam^[15], the shape of the pump beam on the upper surface of a composite ceramic thin-disk is like a hexagon, whose diagonal line length is little shorter than the diameter of a composite ceramic thin-disk. The hexagonal pump beam causes an approximate hexagonal temperature distribution on the upper surface of a composite ceramic thin-disk.

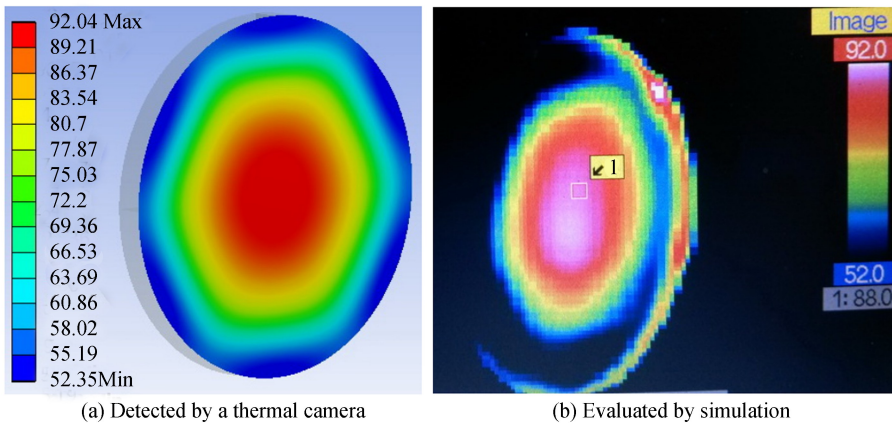


Fig.10 The temperature distributions on the upper surface of a 1200 W pumped composite ceramic thin-disk

The patterns of the temperature distributions as shown in Figs.10 (a) and (b) are very similar to each other. The temperatures of both cases are obviously decreased along the radial direction from the center to the edge of a thin-disk because the pumping area is smaller than the cooling area. However, such two temperature results exhibit no significant changes along the tangential direction because both the pumping and the cooling are quite uniform.

We find that there are some high temperature zones on the edge of a composite ceramic thin-disk in Fig.10 (a), but be absent in Fig.10 (b). That is because the detected temperature with the high value of the edge of the aluminous flange is not true value since the radiation emissivity of ceramic is very different to that of aluminum.

4 Conclusion

In this study, a jet cooling device for a composite ceramic thin-disk laser has been designed, and a systematic simulation model has been developed by using the turbulent heat transfer theory and CFD method. The optimal parameters of a jet cooling device have been obtained with the simulation, and a verification experiment for thermal and I-O power characteristics has been carried out afterward. In the experiment, when the pump power is raised to 1 200 W, the output power of 359 W has been achieved,

and the maximal temperature on the upper surface of the composite ceramic thin-disk detected by a thermal camera reaches 92 °C. The temperature distributions detected by a thermal camera and evaluated by the simulation on the upper surface of a composite ceramic thin-disk are very similar to each other. It has been demonstrated that the simulation model can be employed to precisely evaluate the thermal characteristics of a jet cooling thin-disk composite ceramic laser. It has also been proved that there have been approximate positive linear relationships between the pump power and both the output power and the temperature on the upper surface of the composite ceramic thin-disk. The study is thought to be valuable for the design of a jet cooling composite ceramic thin-disk laser.

References

- [1] JUNG M, RIESBECK T, SCHMITZ J, *et al.* High energy laser demonstrators for defense applications[C]. SPIE, 2016, **10254**: 1025416.
- [2] WANG S, FANG F. High power laser and it's development[J]. *Laser & Optoelectronics Progress*, 2017, **54**(9): 45-58.
- [3] WANG C, CHOW Y, REEKIE L, *et al.* A comparative study of the laser performance of diode-laser-pumped Nd: GdVO₄ and Nd:YVO₄ crystals[J]. *Applied Physics B*, 2000, **70**(6): 769-772.
- [4] ZOU Y, HU M, LI P, *et al.* Temperature characteristics of frequency separation in Nd-doped dual-frequency microchip laser[J]. *Acta Photonica Sinica*, 2019, **48**(6): 0614001.
- [5] CHEN Y, CHEN B, BASSM. Calculation of three-dimensional thermal-gradient-induced stress birefringence in slab lasers[J]. *Applied Physics B*, 2005, **81**(1): 75-82.
- [6] CHENAIS S, DRUON F, FORGET S, *et al.* On thermal effects in solid-state lasers; the case of ytterbium-doped materials[J]. *Progress in Quantum Electronics*, 2006, **30**(4): 89-153.
- [7] WU Y, LONG X, JIAO Z, *et al.* Optimal design of high power Nd : YAG laser based on compensation of thermal lens effect[J]. *Laser Technology*, 2015, **39**(3): 377-380
- [8] YANG H, FENG G, ZHOU S. Thermal effects in high-powerNd : YAG disk-type solid state laser[J]. *Optics & Laser Technology*, 2011, **43**: 1006-1015.
- [9] KOUZNETSOV D, BISSON J. Role of undoped cap in the scaling of thin-disk lasers[J]. *Optical Society of America*, 2008, **25**(3): 338-345.
- [10] VRETENAR N, CARSON T, PETERSON P, *et al.* Thermal and stress characterization of various thin-disk laser configurations at room temperature[C]. SPIE, 2011, **7912**: 79120B.
- [11] SARAVANI M, JAFARNIA A, AZIZI M. Effect of heat spreader thickness and material on temperature distribution and stresses in thin disk laser crystals[J]. *Optics & Laser Technology*, 2012, **44**: 756-762.
- [12] GUO J, JIA K, YANG F, *et al.* Study of jet cooling in disk laser[J]. *High Power Laser and Particle Beams*, 2014, **26**(1): 22-26.
- [13] SHAO N, ZHU X, ZHU G, *et al.* Study on jet array impingement cooling for crystal module of thin disk laser[J]. *Laser Technology*, 2016, **40**(5): 695-700.
- [14] YANG J, WANG X, YANG Q. Advances in jet impinging heattransfer[J]. *Vacuum & Cryogenics*, 2018, **24**(4): 217-222.
- [15] JIA K, JIANG Y, YANG F, *et al.* 340 W average power output of diode-pumped composite ceramic YAG/Nd : YAG disk laser[J]. *Laser Physics*, 2016, **26**: 115801.
- [16] ZHANG X, LIU D, SANG Y. Effects of aging on the characteristics of Nd : YAG nano-powders[J]. *Journal Alloys and Compounds*, 2010, **502**: 206-210.
- [17] SALADINO M, NASILLO G, MARTINO D. Synthesis of Nd : YAG nano-powder using the citrate method with microwave irradiation[J]. *Journal Alloys and Compounds*, 2010, **491**: 737-741.
- [18] ZHANG W, LU T, WEI N. Assessment of light scattering by pores in Nd : YAG transparent ceramics[J]. *Journal Alloys and Compounds*, 2012, **520**: 36-41.
- [19] YANG S, TAO W. Heat transfer[M]. Beijing: Higher Education Press, 2006: 13-15, 43-45, 206-211.
- [20] WANG F. Analysis of compute fluid dynamics-CFD software theory andapplication[M]. Beijing: Qinghua University Press, 2004: 12, 203.